Acta Oceanol. Sin., 2011, Vol. 30, No. 2, P. 25-32
DOI: 10.1007/s13131-011-0102-y
http://www.hyxb.org.cn
E-mail: hyxbe@263.net

Spectral wave transformation model for simulating refraction-diffraction with strongly reflecting coastal structures

ZHENG Jinhai[1,2*], NGUYEN Viet Thanh[1,2], ZHANG Chi[1,2]

[1] State Key Laboratory of Hydrology-Water Resources and Hydraulic Engineering, Hohai University, Nanjing 210098, China

[2] College of Harbor Coastal and Offshore Engineering, Hohai University, Nanjing 210098, China

Received 18 January 2010; accepted 27 September 2010

Abstract
On the basis of the wave action balance equation which incorporates refraction, diffraction, reflection and wave-current interaction, a directional spectral wave transformation model WABED is developed for predicting the irregular wave refraction-diffraction with strongly reflecting structures in coastal regions. In the model, diffraction is taken into account by introducing a term formulated from a parabolic approximation wave equation, and reflection is calculated through a back-marching numerical approach at the reflecting boundary. Two experimental data sets are used to examine the performance of present model with regard to wave characteristics around reflecting coastal structures. One is from a physical experiment at idealized inlet with parallel jetties, while the other is from a laboratory study on a coastal project of the concave breakwater. Reasonably good agreements are found for both cases, revealing the applicability of the present model for predicting combined wave refraction-diffraction processes with strongly reflecting coastal structures.
Key words:

1 Introduction

When waves propagate towards the shore, their transformation processes often change significantly due to the non-uniform bathymetry such as shoaling, refraction, and breaking, with a result of variation and redistribution of wave characteristics. The case could be largely more complicate when coastal structures exist, where wave diffraction and reflection around structures become dominant. For example, the wave reflection would lead to the concentration of wave energy and local scour in front of a detached breakwater, and the wave diffraction can also modify the wave field and topography behind it. At coastal inlets with jetties, the wave reflection and diffraction have an unneglectable impact on the navigation security and channel siltation. As a consequence, reliable wave prediction is of fundamental importance for such coastal engineering, where wave refraction-diffraction associated with strongly reflecting structures play significant role.

Numerical modeling of wave transformation in nearshore regions has been a widely used technique of continuously increasing interest, because of its low-cost and easy-implementation. For decades, remarkable advances in wave modeling have been made with regard to the improvement of model accuracy or physical completeness. On the other hand, all models have own advantages and limitations, with their applicabilitys in coastal engineering depending on a high degree on the site-specific physical processes and the CPU time requirement. At the present state of art, most wave models can be classified into two categories referred as “phase-resolving models” and “phase-averaged models”, respectively. The phase-resolving models calculate detailed wave characteristics with a variety of transformation patterns by solving mass and momentum conservation equations in a time domain. The well-known Boussinesq type models belong to this category (e.g. Peregrine, 1967; Madsen et al., 1991; Wei et al., 1995; Veeramony and Svendsen, 2000). However, phase-resolving models are rather computationally expensive so that their practical applications are always limited to relatively small spatial

Foundation item: The National Natural Science Foundation of China under Grant No.50979033, the Program for New Century Excellent Talents in University of China under Grand No. NCET-07-0255, the Specialized Research Fund for the Doctoral Program of Higher Education under Grant No.20100094110016 and the Special Research Funding of State Key Laboratory of Hydrology-Water Resources and Hydraulic Engineering Grant No.2009585812.
*Correspondence author, E-mail: jhzheng@hhu.edu.cn

dimensions with shallow waters. The phase-averaged models neglect variations in the wave phase in calculating wave and other nearshore processes, but only solving changes of wave averaged physical variables in a frequency-domain based on the wave energy or action balance equation. This type of models is particularly suited for directional wave transformation over large study areas in engineering applications, since they provide the most cared wave parameters with relatively low computational time-consuming. For example, SWAN model (Booij et al., 1999), STWAVE model (Smith et al., 1999) and WABED model (Lin et al., 2008) have been widely used and validated in both deep-ocean and nearshore wave predictions. Reviews of different types of wave prediction models for offshore and coastal engineering applications were presented in Panchang and Demirbilek (1998). As pointed out, the original phase-averaged wave energy (action) balance equations cannot directly represent wave diffraction and reflection. Nevertheless, these processes could be incorporated in such models in approximate ways (Smith et al., 2001; Mase et al., 2005). Various methods have been investigated over the past decade to include diffraction or reflection in phase-averaged wave models (e.g. Rivero et al., 1997; Holthuijsen et al., 2004). However, few studies has been carried out focusing on the spectral wave model performance in simulating combined processes of refraction- diffraction with strongly reflecting structures over an arbitrary bathymetry, which is greatly concerned in practical coastal engineering designs.

The primary purpose of this study is to validate WABED, a spectral random wave transformation model, on the condition that coupled wave refraction and diffraction occur around strongly reflecting coastal structures. The paper is organized in the following way. Section 2 describes the governing equation and the numerical scheme of present model, while the parameterizations of several key factors are outlined as well. Model performances and its appropriateness in coastal applications are examined and discussed though comparisons with experimental data from two physical models consisting of an idealized inlet with parallel jetties and a coastal project with a concave breakwater, as presented in Section 3 and Section 4, respectively. Finally, the concluding remarks are summarized in Section 5.

2 Model Description

2.1 *Governing equation*

The spectral wave transformation model developed in this study is based on the wave action balance equation, which calculates wave characteristics from wave energy density in a phase-average mean hence neglecting the intra-wave variation. Therefore, it is well suited for large-scale computational domains in engineering applications. The capabilities of model include wave shoaling, refraction, diffraction, reflection, depth/current-limited breaking, energy dissipation and wave-current interaction, among which both diffraction and reflection are incorporated in theoretically approximate ways. Wave diffraction is implemented by adding a diffraction term derived from the parabolic wave equation to the energy-balance equation (Mase, 2001). Wave reflection is calculated through a special treatment at the reflecting boundary, which will be shown in the next section. Wave-current interaction is taken into account by considering the Doppler shift in the wave dispersion equation (Zheng and Tang, 2009).

The governing wave action balance equation with the diffraction effect in the model is

$$\frac{\partial(C_xN)}{\partial x}+\frac{\partial(C_yN)}{\partial y}+\frac{\partial(C_\theta N)}{\partial\theta}=\frac{\kappa}{2\sigma}[(CC_g\cos\theta N_y)_y-\frac{1}{2}CC_g\cos\theta N_{yy}]-\varepsilon_bN \quad (1)$$

where N is the wave action density, defined as the wave energy density divided by the angular frequency σ relative to a current. (x, y) are the horizontal coordinates, and θ is the wave direction measured counterclockwise from the x-axis. The first term in the right-hand side of Eq. (1) represents wave diffraction, where κ is the diffraction intensity coefficient and suggested to be 2.5 (Mase, 2001). C and C_g are the wave celerity and the group velocity, respectively. ε_b is a parameterization of wave breaking function for energy dissipation, and a bore based formulation is suggested to parameterize the breaking energy dissipation associated with both depth-variation and ambient currents (Zheng et al., 2008). C_x, C_y, and C_θ are wave velocity components according to x, y, and θ coordinates, respectively, expressed as

$$C_x=C_g\cos\theta+U \quad (2)$$

$$C_y=C_g\sin\theta+V \quad (3)$$

$$C_\theta=\frac{\sigma}{\sin 2kh}(\sin\theta\frac{\partial h}{\partial x}-\cos\theta\frac{\partial h}{\partial y})+\cos\theta\sin\theta\frac{\partial U}{\partial x}-\cos^2\theta\frac{\partial U}{\partial y}+\sin^2\theta\frac{\partial V}{\partial x}-\sin\theta\cos\theta\frac{\partial V}{\partial y} \quad (4)$$

where U and V are the current velocity components in the x and y direction, respectively, and κ is the wave number. The relations between the relative angular frequency σ, the absolute angular frequency ω, the wave number vector k, the current velocity vector U and the water depth h are

$$\sigma^2 = g|\overrightarrow{k}|\tan|\overrightarrow{k}|h \quad (5)$$

$$\sigma = \omega - \overrightarrow{k} \cdot \overrightarrow{U} \quad (6)$$

2.2 *Numerical schemes*

A forward-marching first-order upwind finite-difference method is used to discrete the wave action conservation equation in a staggered rectangular grid system. The wave velocity quantities are stored at boundaries of the wave action density cell, as shown in Fig. 1. Superscripts (i, j, k) and variables $(\delta_x, \delta_y, \delta_\theta)$ are the grid node number and the spatial steps at x, y, and θ coordinates, respectively. Subscript n represents the n-th component of the wave frequency spectrum. The differential equation of Eq. (1) can be written as

$$A_1 N_n^{ijk} + A_2 N_n^{i(j-1)k} + A_3 N_n^{i(j+1)} + A_4 N_n^{ij(k-1)} + A_5 N_n^{ij(k+1)} = -B N_n^{(i-1)jk} \quad (7)$$

where A_1, A_2, A_3, A_4, A_5 and B are known as physical quantities related to wave velocities and energy dissipation with respect to a specific calculation cell.

The Gauss-Seidel method is employed to solve the Eq. (7). Once the seaward boundary condition is given, wave characteristics are calculated in the wave propagation direction through a column-to-column approach. In particular, model can perform the backward marching for seaward reflection in front of a reflecting coastal structure after completing the forward marching computation, on the condition that the angel of structure boundary and wave direction are known together with a reflection coefficient. For both forward and backward marching calculations, a quadratic upstream interpolation of convective kinematics is used in the discretization to reduce numerical diffusion.

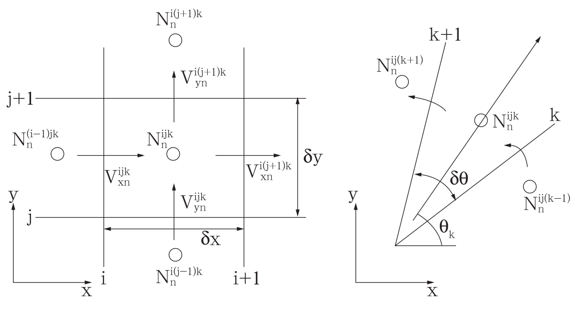

Fig.1. Layout of variables in the cell.

2.3 *Diffraction*

The incorporation of diffraction effect is achieved through adding a diffraction term into the wave action balance equation, as firstly derived from the parabolic wave equation by Mase (2001).

A basic form of the parabolic wave equation including a dissipating term can be written as

$$2ikCC_gA_x + i(kCC_g)_xA + (CC_gA_y)_y = -ikC\varepsilon_bA \quad (8)$$

where k is the wave number and A is the complex amplitude. Assuming the wave energy E equal to $|A|^2$ and $A_yA_y^*$ approximating by $E_{yy}/4$, resulting equations are yielded as following after a series of transformations

$$(C_gE)_x = -\varepsilon_bE \quad (9)$$

$$(CC_gE_y)_y - CC_gE_{yy}/2 \cong 0 \quad (10)$$

Comparing Eqs (9) and (10) with the original wave energy balance equation and replacing energy density E by action density N, the diffraction term introduced into the modified energy equation can be defined as

$$\frac{\kappa}{2\sigma}[(CC_g\cos^2\theta N_y)_y - \frac{1}{2}CC_g\cos^2\theta N_{yy}] \cong 0 \quad (11)$$

The optimized value of the diffraction coefficient κ should be estimated from laboratory or field data (Chen et al., 2010).

2.4 *Reflection*

For reflecting boundary, the backward-marching computations modify the source of the spectral wave action density at cells adjacent to the sea area. The mathematical formulas for reflection in x and y directions are

$$N(x + \Delta x, y, f, \pi - \theta + 2\alpha) = K_{rc}^2N(x, y, f, \theta) \quad (12)$$

$$N(x, y + \Delta y, y, f, -\theta + 2\alpha) = K_{rc}^2N(x, y, f, \theta) \quad (13)$$

where K_{rx} and K_{ry} are reflection coefficients in x and y directions, respectively. α is the angel of the normal line to the structure from the x-axis in Eq. (12), and the angel of the structure from the x-axis in Eq. (13), respectively. Note that, the input of inclination angel of reflecting structure is crucial for calculating reflected waves in backward marching computations, since it provides the reasonable direction of reflected wave energy which can not be implied locally on rectangular grids (Mase et al., 2005).

3 Application to an idealized inlet with parallel jetties

3.1 *Outline of experimental study*

Model was first tested with an experimental study (Seabergh et al., 2005) on wave refraction, diffraction and reflection at an idealized inlet with two parallel jetties. Figure 2 shows the depth contour lines of laboratory bathymetry and locations of parallel jetties. In particular, two different jetty types, fully absorbing and fully reflecting, are constructed to evaluate the wave climate associated with two different reflecting rates of jetties. Incident regular waves were unidirectional and 20° oblique to shore-normal. Table 1 lists the tested incident wave conditions. Wave height was measured on the up-wave side of the south jetty and inside the inlet from a linear array of capacitance wave gauges, of which the locations are shown as circles in Fig. 3. Five transect lines for model to data comparisons are also shown.

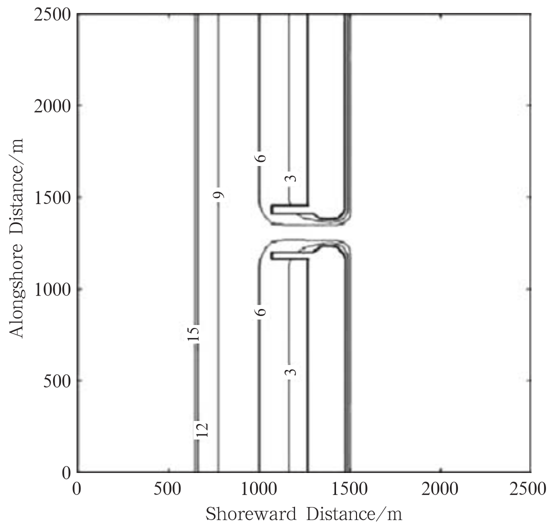

Fig.2. Depth contours of physical model.

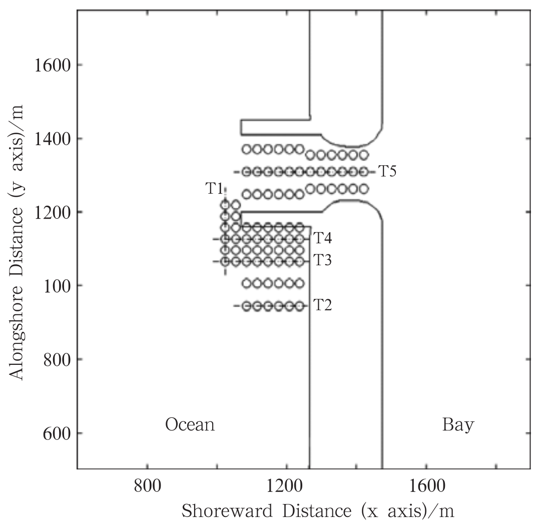

Fig.3. Locations of wave gauges (circle) and transect lines (dashed lines).

Table 1. Experimental conditions for an idealized inlet with parallel jetties (1:50 scale)

Jetty type	Wave height/m	Wave period/sec	Wave direction(°)	Wave type
Fully absorbing	2.0	11	–20	Regular
Fully reflecting	2.0	11	–20	Regular

3.2 *Model to data comparison*

For the fully absorbing and reflecting conditions, the present wave model was run with both reflection coefficients set to be 0 and 1, respectively. The diffraction coefficient κ was determined to be its recommended value of 2.5 (Mase, 2001) for both cases, since no more measured data was available for verification. The calculated wave heights along transect lines T1-T4 were compared with measured data, as shown in Fig. 4 (fully absorbing case) and Fig. 5 (fully reflecting case). As displayed, the model predicted well the variation pattern of wave heights along all transect lines. An obvious enhancement of wave heights is found at the up-wave side of the reflecting jetty (Fig. 5), which becomes larger with a decreasing distance from the jetty. This feature is also captured well by the model, although the peak wave heights are underestimated at most transect lines. For complement, Tab. 2 lists the calculated mean statistical errors of wave height and wave direction between numerical results and experimental data. It can be observed that model predicts both wave height and direction in a generally good manner for both cases, hence supporting the capability of present model for predicting the complex wave climate with strongly reflecting structures in coastal applications.

4 Application to a project with concave breakwater

4.1 *Outline of experimental study*

Laboratory experiment (Zheng et al., 2006) was conducted in a wave basin of 50 m long and 17.3 m wide at Hohai University to study wave characteristics in front of the breakwaters with a concave angle of 152°. The physical model was initially designed to provide a basis for a project of prolonging breakwater in the Shengsi Central Fishery Harbor in the Zhoushan Archipelago, Zhejiang Province, with a model scale of

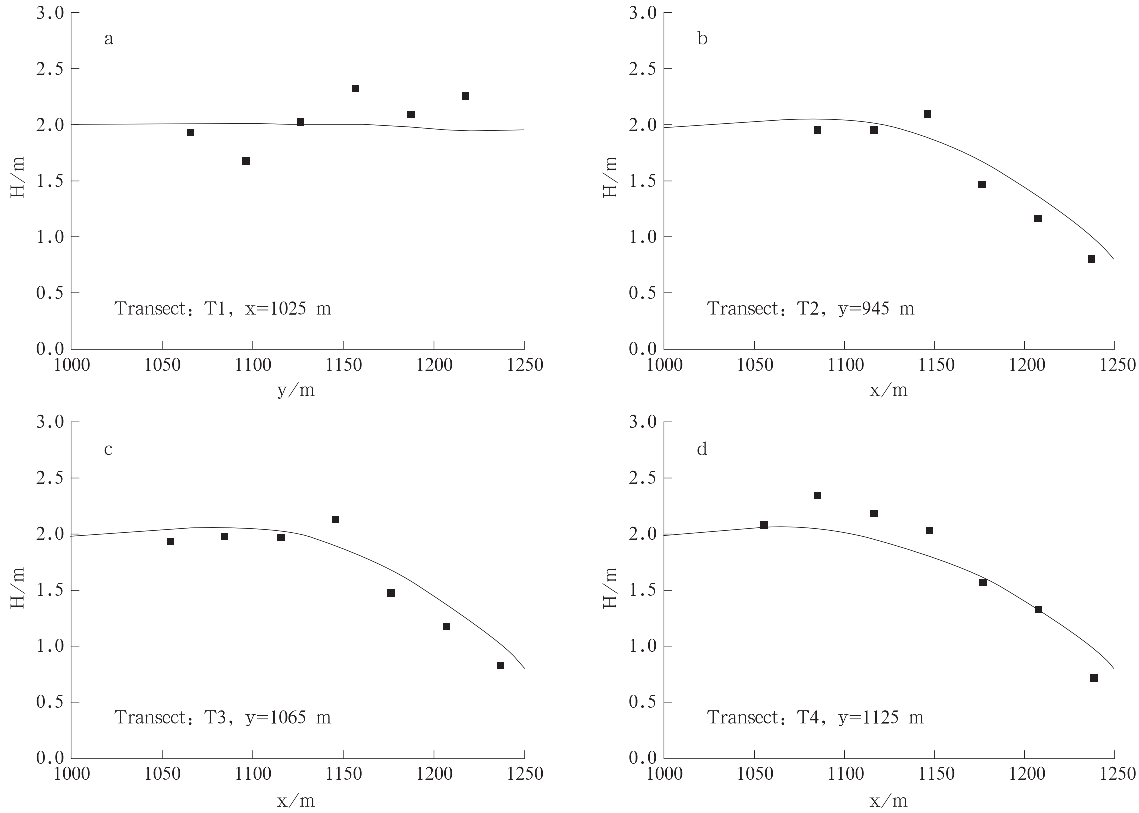

Fig.4. Comparisons of wave height between experimental data (dot) and model results (line) along four transects with fully absorbing jetties.

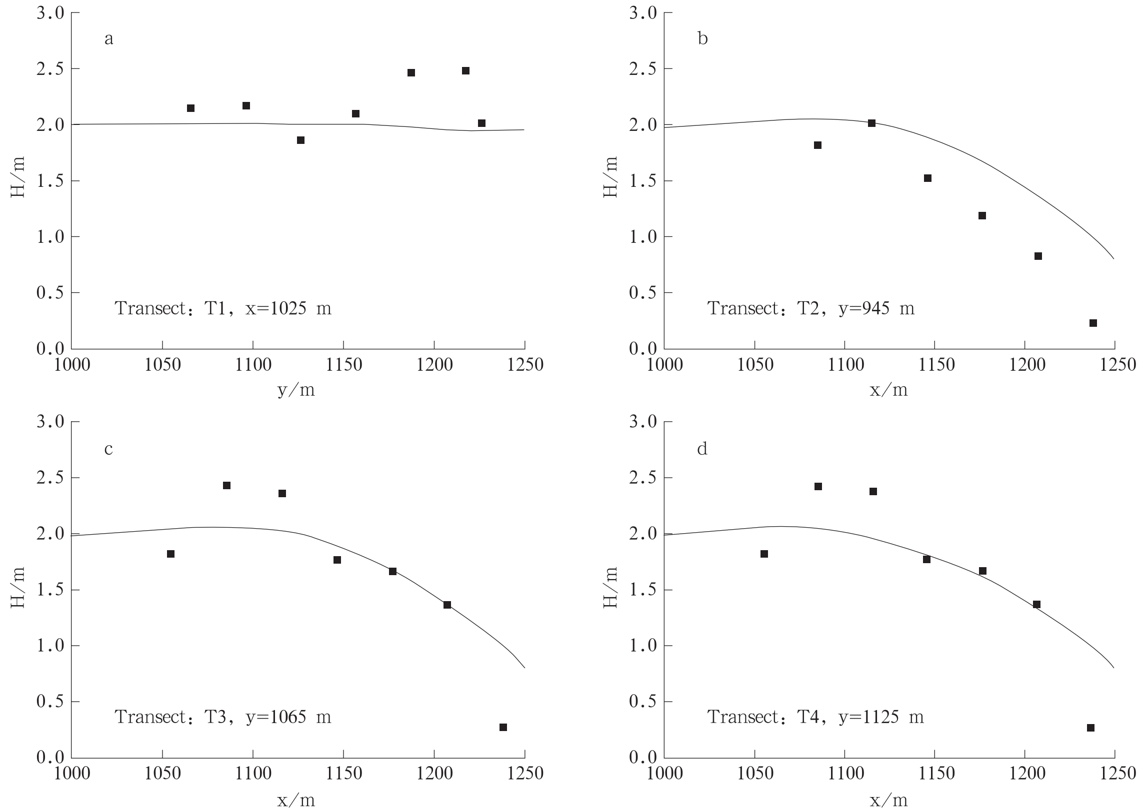

Fig.5. Comparisons of wave height between experimental data (dot) and model results (line) along four transects with fully reflecting jetties.

1:80. 50-year's return period incident random waves in the directions of ENE and E were generated by a hydraulically driven piston-type wave machine at one end of the wave basin referred to the JONSWAP spectrum, under three water depths corresponding to the extreme high sea level, designed high sea level, and extreme low sea level, respectively. 26 pieces of the electric-capacity wave gauge were set in front of the concave breakwaters, while 10 pieces were set at the gap. Fig. 6 shows the layout of physical model and locations of wave gauges. The test conditions are listed in Tab. 3.

4.2 *Model to data comparison*

Figure 7 shows the comparison between predicted and observed wave heights at 36 measuring points under three water levels. Reasonably good agreements are found. Model accurately simulated the amplification of wave height in front of the concave breakwater due to the superposition of incident waves upon reflected waves and the diffraction behind the breakwater. The influence range of reflection becomes larger with the increase of the water level, which is underestimated by the numerical model to a little extent. The wave diffraction behind the breakwater is slightly underpredicted either. As calculated, the mean values of absolute relative wave height errors under high, medium and low water level are 24.5%, 22.3% and 22.1%, respectively. Those disagreements seem to be

Table 2. Statistical mean errors of calculated wave height and direction

Jetty type	Mean of Absolute Relative Wave Height Error (%)	Mean of Absolute Wave Height Error/m	Mean of Absolute Wave Direction Error(°)
Fully absorbing	16.6	0.30	7.6
Fully reflecting	33.9	0.25	9.5
Average	25.3	0.28	8.6

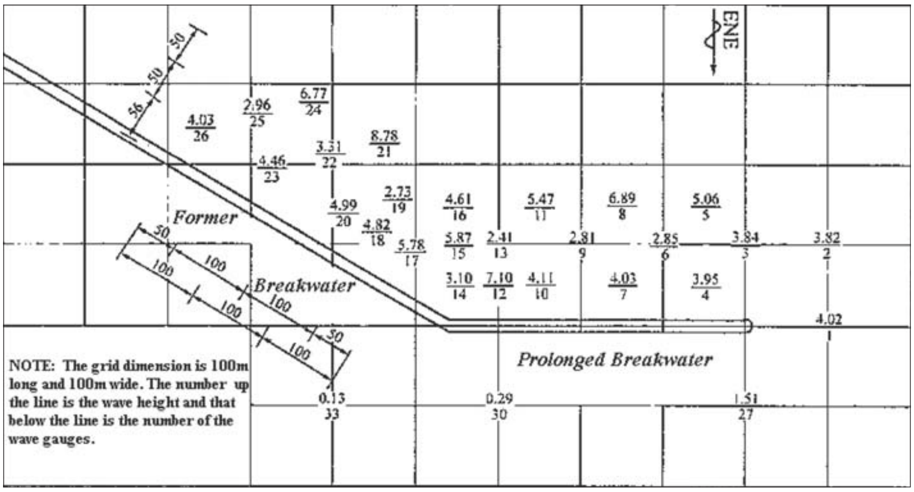

Fig.6. Layout of physical model and locations of wave gauges.

Table 3. Experimental conditions for a project with concave breakwater (1:80 scale)

Wave direction	sea level/m	Water depth/m	Wave height/m	Peak wave period/s	Wave type
	+3.01	9.01	5.76		
ENE	+2.05	8.05	5.15	15.6	Irregular
	–1.76	4.24	2.71		
	+3.01	9.01	5.18		
E	+2.05	8.05	5.15	13.7	Irregular
	–1.76	4.24	2.49		

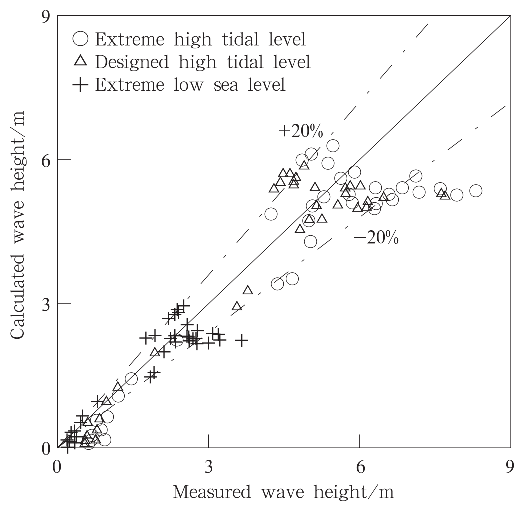

Fig.7. Comparison between measured and calculated wave heights around the concave breakwater under three water levels.

more obvious under higher water level, which may be attributed to the wave-wave interaction not accounted in the present model. Nevertheless, overall deviations are considered acceptable (the mean error for all three water levels is 23% and the correlation coefficient is 0.936), when the uncertainty of the complex wave-structure interaction and the relatively convenient numerical implementation are taken into account. It is demonstrated that the present model could provide fairly good performance on simulating the coupled wave refraction-diffraction processes around a reflecting structure with an irregular shape.

5 Conclusions

A spectral wave transformation model is developed to investigate the random wave refraction-diffraction processes with strongly reflecting coastal structures. Based on the wave action balance equation, the wave diffraction and reflection are incorporated through theoretical approximations to enhance the model capabilities. Two experimental data sets are used to evaluate the model application on dealing with combined wave refraction-diffraction around reflecting structures in coastal regions. One was from a laboratory study on wave characteristics at an idealized inlet with parallel jetties of absorbing or fully reflecting type. The other was collected in a physical model conducted for a coastal project of the concave breakwater with an angle of 152°. Comparisons of model results and experimental data show overall good agreements for both cases, indicating that the present model is capable of describing wave refraction-diffraction processes with a wide range of reflecting structures in coastal applications. It implies the confidence that the model will almost certainly perform reasonably well within the proper range of applications where diffraction and reflection are significantly less relevant, because the model performs reasonably well in these conditions.

References

Booij N, Ris R C, Holthuijsen L H. 1999. A third-generation wave model for coastal regions. 1. Model description and validation. Journal of Geophysical Research, 104(C4): 7649–7666

Chen Xiaowen, Zheng Jinhai, Zhang Chi. 2010. Evaluation of diffraction predictability in two phase averaged wave models. China Ocean Engineering, 24(2): 235–244

Holthuijsen L H, Herman A, Booij N. 2004. Phase-decoupled refraction-diffraction for spectral wave models. Coastal Engineering, 49(4): 291–305

Lin L, Demirbilek Z, Mase H, et al. 2008. CMS-Wave: A nearshore spectral wave processes model for coastal inlets and navigation projects. Coastal Inlets Research Program, Coastal and Hydraulics Laboratory Technical Report ERDC/CHL-TR-08-13. U.S. Army Engineer Research and Development Center, Vicksburg, Mississippi, USA

Madsen P A, Murray R, Sorensen O R. 1991. A new form of the Boussinesq equations with improved linear dispersion characteristics. Coastal Engineering, 15(4): 371–388

Mase H. 2001. Multi-directional random wave transformation model based on energy balance equation. Coastal Engineering Journal, 43(4): 317–337

Mase H, Oki K, Hedges T, et al. 2005. Extended energy balance equation wave model for multidirectional random wave transformation. Ocean Engineering, 32(8-9): 961–985

Peregrine D H. 1967. Long waves on a beach. Journal of Fluid Mechanics, 27(4): 815–827

Panchang V, Demirbilek Z. 1998. Wave prediction models for coastal engineering applications. Wave Phenomena and Offshore Topics, Chapter 4 in Developments in Offshore Engineering, Gulf Publishing Co, Houston, TX, 163–194

Rivero F J, Arcilla A S, Carci E. 1997. An analysis of diffraction in spectral wave models. Proceedings 3rd Intl. Symp. of Ocean Wave Measurement and Analysis, Waves'97, ASCE, 431–445

Smith J M, Resio D T, Zundel A. 1999. STWAVE: Steady-state spectral wave model, Report 1, user's manual for STWAVE version 2.0. Instruction Report CHL-99-1, U S. Army Engineer Waterways Experiment Station, Vicksburg, MS

Smith J M. 2001. Breaking in a spectral wave model. Proceedings of the Fourth International Symposium of Ocean Wave Measurement and Analysis, Waves 01, ASCE, San Francisco, CA, USA, 1022–1031

Seabergh W C, Lin L, Demirbilek Z. 2005. Laboratory study of hydrodynamics near absorbing and fully reflecting jetties. Coastal Inlet Research Program, Technical Report ERDC/CHL-TR-05-8, U.S. Army Engineer Research and Development Center, Vicksburg, MS

Veeramony J, Svendsen I A. 2000. The flow in surf-zone waves. Coastal Engineering, 39(2-4): 93–122

Wei G, Kirby J T, Grilli S T, et al. 1995. A fully nonlinear Boussinesq model for surface waves. 1. Highly nonlinear unsteady waves. Journal of Fluid Mechanics, 294: 71–92

Zheng Jinhai, Tang Yu. 2009. Numberical simulation of spatial between wave breaking point and location of maximum wave-induced current. China Ocean Engineering, 23(1):59–71

Zheng Jinhai, Qian Jin, Zhong Husui, et al. 2006. Three-dimensional physical study on wave characteristics in front of concave breakwaters. Proceedings of the second Chinese-German Joint Symposium on Coastal and Ocean Engineering, 100–106

Zheng Jinhai, Mase Hajime, Demirbilek Zeki, et al. 2008. Implementation and evaluation of alternative wave breaking formulas in a coastal spectral wave model. Ocean Engineering, 35(11–12): 1090–1101